ELSEVIER

International Journal of Mass Spectrometry 209 (2001) 113–124

www.elsevier.com/locate/ijms

# Secondary ion yield improvements for phosphated and sulfated molecules using substrate-enhanced time-of-flight secondary ion mass spectrometry

Robert D. English[a,b], Michael J. Van Stipdonk[a,c], Emile A. Schweikert[a,*]

[a]*Department of Chemistry, P.O. Box 30012, Texas A&M University, College Station, Texas 77843-3012*
[b]*Department of Pharmacology & Molecular Sciences, Johns Hopkins University, School of Medicine, Baltimore, Maryland 21205*
[c]*Department of Chemistry, Wichita State University, Wichita, Kansas 67260-0051*

Received 6 February 2001; accepted 18 May 2001

**Abstract**

Aminoethanethiol (AET), at an appropriate pH, forms a charged self-assembled monolayer (SAM) on Au surfaces. We have shown that an AET-SAM can be used to adsorb organic and inorganic anions from aqueous and ethanol solutions. The adsorbed anions can then be sputtered with high efficiency for characterization by time-of-flight secondary ion mass spectrometry. We present here the application of the AET monolayer for the characterization of more complex and biologically relevant organic sulfates and phosphates up to 1150 Daltons, each featuring a charged anionic site to facilitate the adsorption to the monolayer by ion-pair formation. We monitored the mass spectra and secondary ion emission following 20 keV $(CsI)_nCs^+$ ($n$=0–2) projectile impacts on targets composed of thin layers deposited on Si, Au, and AET/Au substrates; and of thick targets (thick with respect to the 10–100 nm range of projectile). For each molecule used in this study, the secondary ion yield increased when the anion was deposited as a thin layer, relative to a thick layer, and is greatest for AET/Au substrates compared to bare Au and polished Si substrates. Additionally, the intact-to-fragment ion yield ratio is lower when sputtering from the solid salt target than from the AET monolayer. (Int J Mass Spectrom 209 (2001) 113–124) © 2001 Elsevier Science B.V.

*Keywords:* Time-of-flight-secondary ion mass spectrometry; Self-assembled monolayer; Phospholipids; Anions; Aminoethanethiol

## 1. Introduction

Several authors have demonstrated that secondary ion yields in organic secondary ion mass spectrometry (SIMS) can be improved by using polyatomic primary ions as projectiles [1–10]. To further improve the performance of time-of-flight (TOF)-SIMS for organic molecular characterization, we have investigated novel substrates that allow the collection and concentration of classes of analyte for subsequent interrogation by TOF-SIMS. We have shown in previous studies that SIMS detection sensitivity for organic and inorganic anion analytes can be enhanced by several orders of magnitude when these species are deposited onto or adsorbed to an aminoethanethiol (AET) self-assembled monolayer (SAM) on Au [11–13]. Our experiments followed earlier studies in

*Corresponding author. E-mail: schweikert@mail.chem.tamm.edu


*PII* S1387-3806(01)00468-7

which AET substrates were used to adsorb nucleotides for characterization via SIMS [14] and to remove salt and other contaminants during sample preparation for matrix-assisted laser desorption ionization (MALDI) [15].

The purpose of the present study was to extend our previous experiments into the realm of biomolecules and to determine whether depositing the analyte onto AET could also enhance detection of higher mass molecular anions via TOF-SIMS. We present below a comparison of the secondary ion emission generated from phospholipids and sulfated organic molecules deposited on Si, Au, and AET/Au substrates and sputtered by $(CsI)_nCs^+$ ($n = 0–2$) projectiles. Further topics investigated include the reversibility of anion adsorption to the AET monolayer and the ratio of intact ion (unfragmented molecule ions) to prompt fragment ion signal generated by atomic and polyatomic primary ions.

## 2. Experimental section

### 2.1. Materials

Si wafers (4 in, PB100) were purchased from Wafer World, Inc. (W. Palm Beach, Florida). The wafers were coated with a 10 nm Ti adhesion layer followed by a 200 nm thick layer of Au (Lance Goddard Associates, Forest City, California). The name, acronym, molecular weight, and structure (used to identify intact anion ion peaks in the mass spectra displayed in Figs. 1–5) for each anion used in this study are provided in Table 1. Brain sulfatide (BS, >99%), lysophosphatidic acid (OGP, >99%), myristoyl lysobiphosphatidic acid (LBPA, >99%), 1-stearoyl-2-oleoyl-SN-glycero-3-[phospho-rac-1-glycerol] (SOGP, >99%), and 1,2-dipalmitoyl-SN-glycero-3-phosphoethanolamine-N-(7-nitro-2-1,3-benzoxadiazol-4-yl) (DGPNB, >99%) were purchased from Avanti Polar Lipids, Inc. (Alabaster, Alabama). Cholecystokinin octapeptide-{26–33} (CCK8) was purchased from California Peptide Research, Inc. (Napa, California). 2-aminoethanethiol hydrochloride (AET) was purchased from Aldrich Chemical (Milwaukee, Wisconsin). High purity ethanol (EtOH) was purchased from AAPER Alcohol and Chemical Co. (Shelbyville, Kentucky). Chloroform, 99%, was purchased from Fisher Scientific (Pittsburgh, Pennsylvania). All chemicals were used as received. The water used in these experiments was purified with a Milli-Q (Millipore) deionization system.

### 2.2. Monolayer preparation

The Au coated Si wafers were cut into 1 $cm^2$ pieces using a diamond scribe, rinsed with EtOH and ozone cleaned for 10 min under UV light. To prepare SAM surfaces, the Au on Si substrates were immersed in 1 mM solutions of AET in EtOH and left to soak for 18 h. The monolayer coated substrates were removed from the thiol solution, rinsed with EtOH, rinsed with 0.1 M HCl to ensure protonation of the terminal amine, rinsed with Milli-Q water to remove excess chlorine, and dried with a stream of dry nitrogen.

### 2.3. Preparation of surfaces with adsorbed anions

Two procedures were used to produce AET monolayer, Au on Si and polished Si surfaces with adsorbed phospholipids or organic sulfates. In procedure **(1)**, 10 $\mu$L aliquots of the respective anions in chloroform [or 3:1 EtOH:water for CCK8] (solution concentration was 1 mg/mL) were pipetted directly onto individual AET monolayer/Au substrates. The chloroform or EtOH:water mixture was allowed to evaporate in air, leaving a visible film, and the surface was subsequently rinsed with 1 mL of solvent to remove loosely bound material. The wafers were then allowed to dry in a fume hood and were mounted to the sample support for the mass spectrometer using double-sided tape.

In procedure **(2)**, the instrumental limit of detection was tested for LBPA adsorbed onto AET surfaces. The sample preparation consisted of drying 10 $\mu$L aliquots of LBPA solution onto AET substrates without the additional chloroform rinse step. The concentration of the solutions was adjusted so that the total sample load applied to the surface ranged from 1 nmol–1 fmol. At 1 nmol, coverage of the substrate was estimated to be $\sim 10^{14}$ LBPA anions/$cm^2$, corresponding to at most

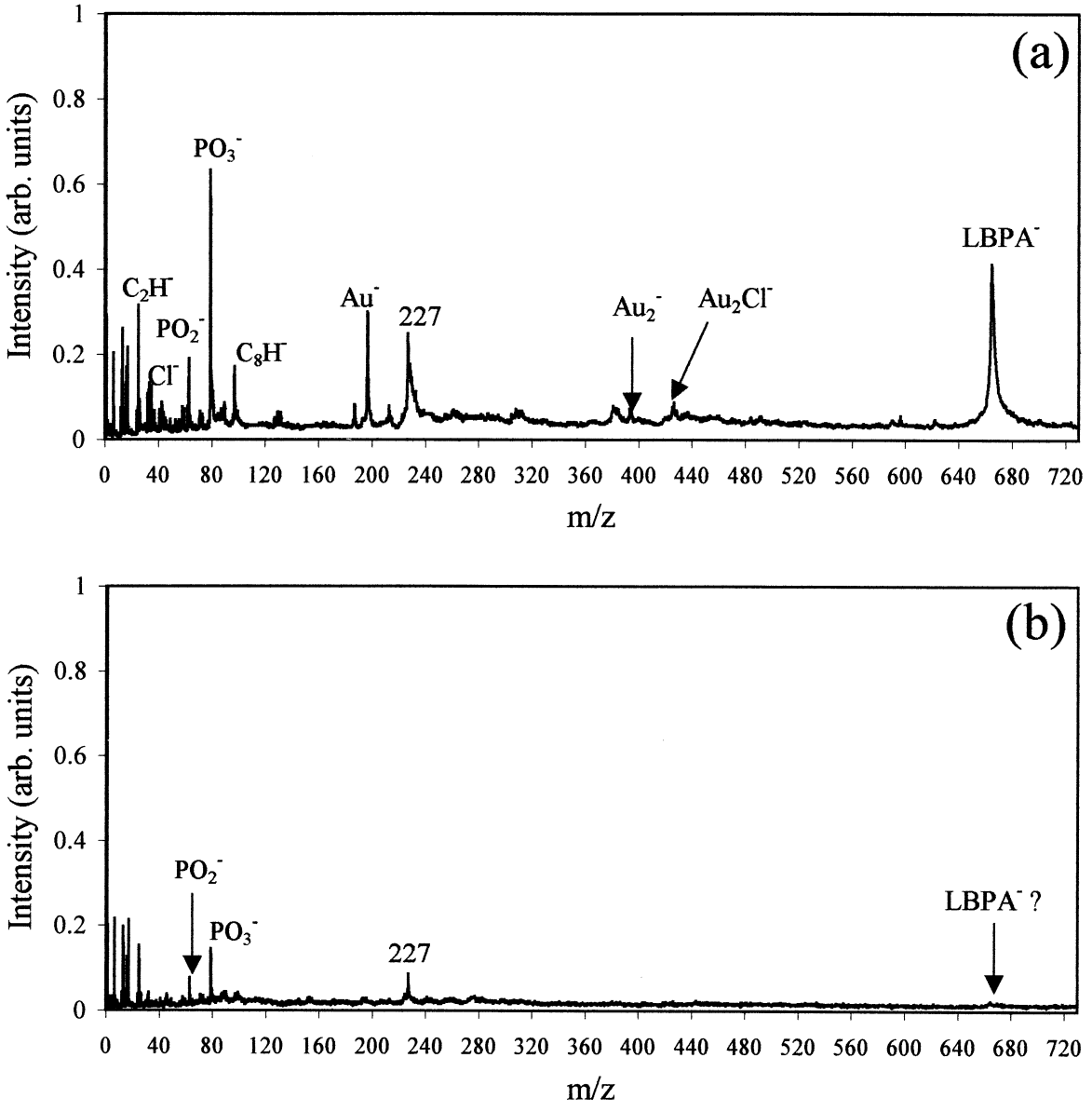


Fig. 1. Negative secondary ion mass spectra of an AET monolayer on Au: (a) following rinse with 8 mL of 0.1 M HCl, rinse with 8 mL Milli-Q water, and the application of LBPA as described for procedure **(1)** (see Sec. 2) and (b) thick LBPA. The spectra were acquired for 45 min each using 20 keV $Cs^+$ projectiles at a dose of $\sim 3 \times 10^4$ ions. The ion intensities in both spectra are corrected for the number of incident primary ions.

one monolayer coverage. However, we have not performed any studies to confirm the coverage.

For phospholipid anion reversibility experiments, procedure **(1)** and the following process were used when rinsing phospholipids from the substrate and applying a new phospholipid mixture. The anion-coated AET substrate was removed from the instrument, rinsed with 8 mL of 0.1 M HCl, 8 mL of Milli-Q water (to remove adsorbed $Cl^-$), and dried with a stream of dry $N_2$ gas. Next, 10 $\mu$L of a 50:50

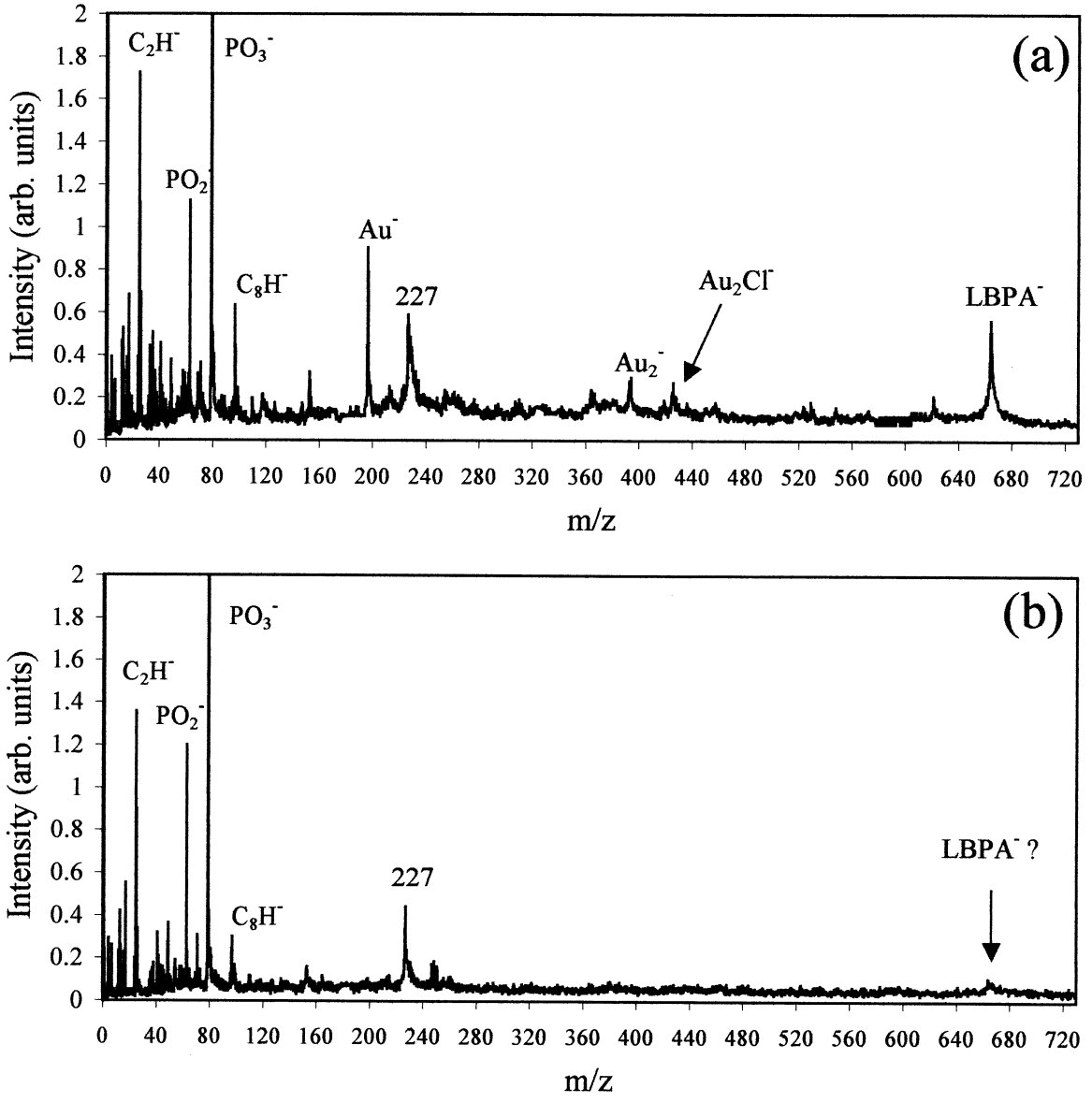


Fig. 2. Negative secondary ion mass spectra of: (a) LBPA thin layer on AET as described for procedure **(1)** (see Sec. 2) and (b) thick LBPA. The spectra were acquired for 45 min each using 20 keV $(CsI)Cs^+$ projectiles at a dose of $\sim 1 \times 10^4$ ions. The ion intensities in both spectra are corrected for the number of incident primary ions.

phospholipid mixture was applied to the monolayer surface (the relative concentrations were arbitrarily chosen), allowed to dry, and rinsed with 1 mL of chloroform to remove unbound material. The monolayer substrate was blown dry with $N_2$ gas and reinserted into the mass spectrometer.

### *2.4. Thick target preparation*

Mass spectra were also collected from targets dried from solution onto stainless steel backings. In contrast to the exchanged monolayer samples, these targets are considered infinitely thick relative to the range of the

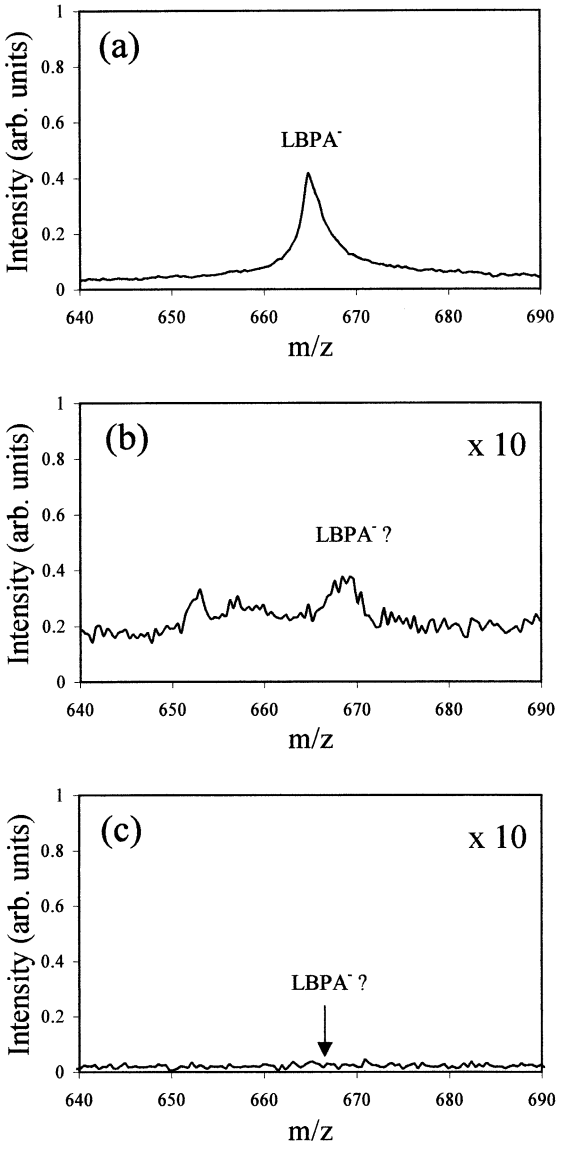


Fig. 3. Negative secondary ion mass spectra of: (a) LBPA thin layer on AET, (b) LBPA on a Au on Si blank substrate (no monolayer present), (c) LBPA on polished Si substrate. The adsorbed surfaces were all prepared using procedure **(1)** (see Sec. 2). The spectra were acquired for 40 min each using 20 keV $Cs^+$ projectiles at a dose of $\sim 3 \times 10^4$ ions. The ion intensities in both spectra are corrected for the number of incident primary ions.

primary ion (~10–100 nm). To prepare thick samples, 1 mg/mL solutions of the respective molecules were prepared in chloroform, except when noted otherwise. A 50 $\mu$L aliquot of solution was applied to a stainless steel sample support (1.5 × 2 cm) and allowed to dry at room temperature in a fume hood. The solution concentration was chosen empirically to produce thin, homogeneous coverage of the sample support with minimal crust formation. The sample supports were then inserted into the mass spectrometer for analysis.

### 2.5. Mass spectrometry

Negative ion mass spectra were collected using a custom dual TOF-SIMS instrument. The configuration and operation of the instrument have been described elsewhere [2]. $Cs^+$, $(CsI)Cs^+$, and $(CsI)_2Cs^+$ primary ions with an incident energy of 20 keV were used to bombard the various targets at an impact angle of ~27° relative to the surface normal (determined by the geometry of the instrument and primary ion deflection due to the negative acceleration potential applied to the target). Unless stated otherwise, acquisition times were 40–45 min. These experiments were performed using event-by-event bombardment/detection, pulse counting, and a coincidence counting data collection protocol. The experimental approach for the measurement of relative secondary ion yields also has been described elsewhere [2].

Secondary electron emission from the sample target was used to measure the number of incident primary ions. Relative secondary ion yields were calculated by dividing the integrated peak area produced by a particular primary ion by the integrated secondary electron peak from the same projectile. The relative yields are a measure of the number of secondary ions detected per incident primary ion without correction for the ion transmission and detection efficiencies of the instrument. The ion intensities in each mass spectrum were corrected for the number of incident projectiles and the spectra, consequently, also reflect the relative ion yields. The event-by-event bombardment/detection mode and coincidence counting protocol used in these experiments allowed atomic and polyatomic projectile impacts on a particular sample surface to be compared both simultaneously and under the same experimental conditions.

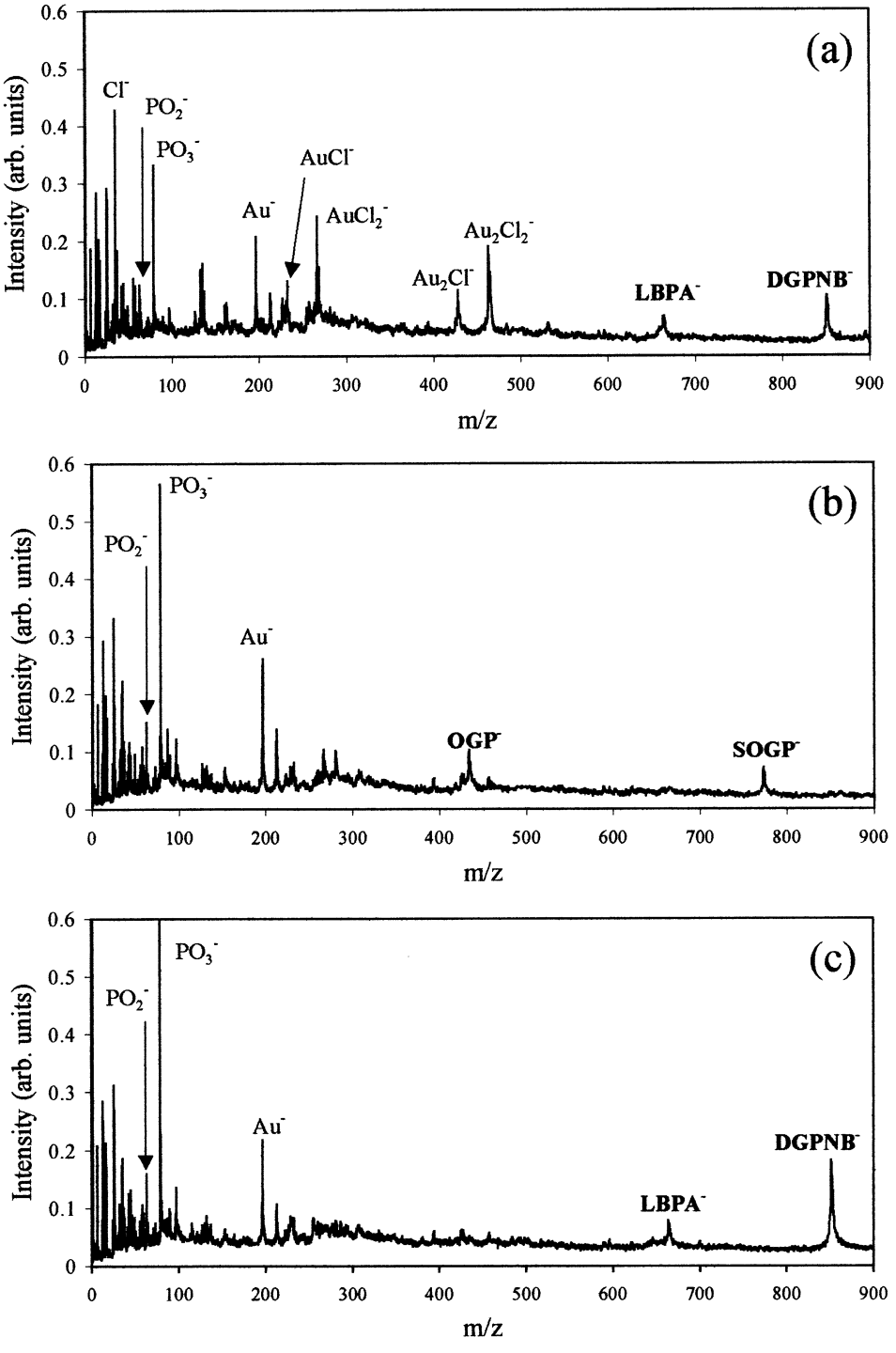


Fig. 4. Negative secondary ion mass spectra produced from the same AET monolayer on Au: (a) following application of 10 $\mu$l of a 50:50 mixture of LBPA and DGPNB in chloroform as described in the text, (b) following rinse with 8 ml of 0.1M HCl and 8 mL water and exposure to a 50:50 mixture of OGP and SOGP as explained in the text, and (c) following rinse with 8 mL of 0.1M HCl and 8 mL water, and exposure to 10 $\mu$l of a 50:50 mixture of LBPA and DGPNB as described in the text. The spectra were acquired for 40 min each using 20 keV $Cs^+$ projectiles at a dose of $\sim 3\times10^4$ ions. The ion intensities in the spectra are corrected for the number of incident primary ions.

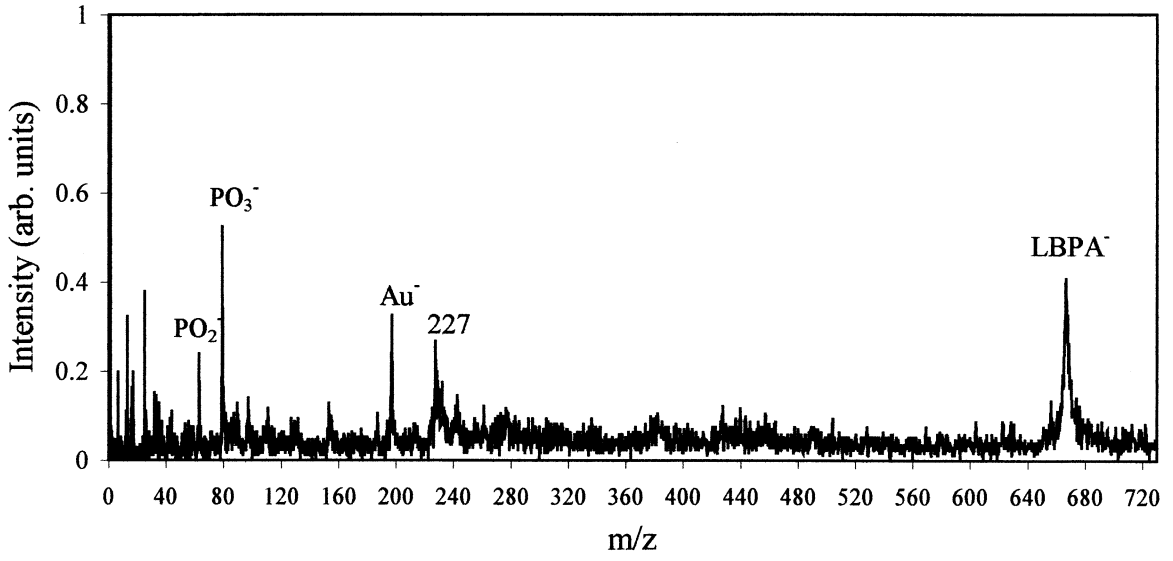


Fig. 5. Negative secondary ion mass spectra of an LBPA-exchanged AET monolayer. The spectrum was acquired in one minute using 20 keV $Cs^+$ projectiles at a dose of $\sim 1 \times 10^3$ ions. The ion intensities in the spectrum are corrected for the number of incident primary ions.

## 3. Results and discussion

### *3.1. Mass spectra produced from aminoethanethiol monolayer, Au on Si, and polished Si substrates*

Fig. 1 shows two negative ion mass spectra generated by 20 keV $Cs^+$ primary ions (dose: $\sim 3 \times 10^4$ ions). Fig. 1(a) shows the spectrum collected from an AET monolayer coated with LBPA as described for procedure **(1)** in the experimental section. The peaks present at mass to charge ratio (*m/z*) 35 and 37 $\{Cl^-\}$, and 429 and 431 $\{Au_2Cl^-\}$ indicate the adsorption of chloride ion to the (positively charged) AET monolayer surface. The uptake of LBPA by the monolayer surface is demonstrated by the prominent peak at *m/z* 666, corresponding to the intact LBPA phospholipid anion, as well as fragment ion peaks at *m/z* 63 and 79 ($PO_2^-$ and $PO_3^-$, respectively). The peak at *m/z* 227 indicates a fragment formed from cleavage of the phospholipid hydrocarbon backbone between the second and third carbon atoms near the phosphate group. Each side of a LBPA molecule has this cleavage site available. Other peaks in the spectrum include $C_2H^-$ and $C_8H^-$ (presumably due to pump oil and/or ion impact induced degradation of the sample), and $Au^-$ and $Au_2^-$ from the Au-coated Si substrate. For comparison, Fig. 1(b) shows a negative ion mass spectrum collected from a thick deposit of LBPA. Lower yields are obtained for $PO_2^-$, $PO_3^-$, and fragment ion at *m/z* 227, and there is a negligible peak at *m/z* 666 for the intact LBPA phospholipid anion.

The mass spectra produced by 20 keV $(CsI)Cs^+$ projectile impacts on the same surfaces are provided in Fig. 2. In Figs. 1 and 2, the ion intensities have been normalized to the number of incident primary ions (the respective ion doses are provided in the figure captions), thus allowing comparison between the figures and providing an indication of the ion yields generated from the different targets by the atomic and polyatomic primary projectiles. Using 20 keV $Cs^+$ primary ions, the yield of the intact LBPA anion was improved by a factor of 55 using the AET substrate over the thick target. When the $(CsI)Cs^+$ cluster was used as the incident projectile, the intact LBPA ion signal using the AET substrate was improved by a factor of 9.

The mass spectra provided in Figs. 1 and 2 are representative of those produced by 20 keV $Cs^+$ and $(CsI)Cs^+$ primary ions when LBPA was adsorbed to the AET monolayer on Au surface. We suggest that

Table 1
Name, acronym, molecular weight, and structure (used to identify intact anion peaks in the mass spectra displayed in Figs. 1–5) for each anion used in this study; molecular weight values shown are for the sodium or ammonium salts; molecular weights of the anions adsorbed to AET surfaces will be 23 or 18 Daltons, respectively, lower than the values listed

| *Name* | *Acronym* | *Molecular Weight* | *Structure* |
|---|---|---|---|
| Lysophosphatidic Acid, (Na salt) | OGP | 458.51 | 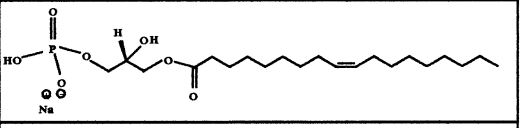 |
| Myristoyl Lysobiphosphatidic Acid, ($NH_4$ salt) | LBPA | 683.90 | 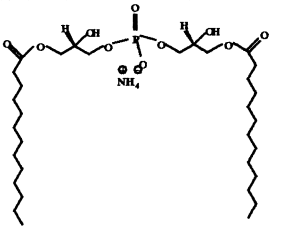 |
| 1-Stearoyl-2-Oleoyl-SN-Glycero-3-[Phospho- rac-(1-glycerol], (Na salt) | SOGP | 799.05 | 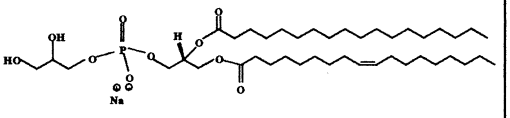 |
| 1,2-dipalmitoyl-SN-Glycero-3-Phosphoethanolamine-N-(7-nitro-2-1, 3-benzoxadiazol-4-yl), ($NH_4$ salt) | DGPNB | 854.05 | 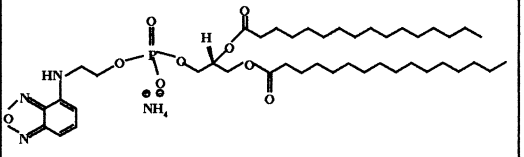 |
| Brain Sulfatide, ($NH_4$ salt) | BS | 907 | 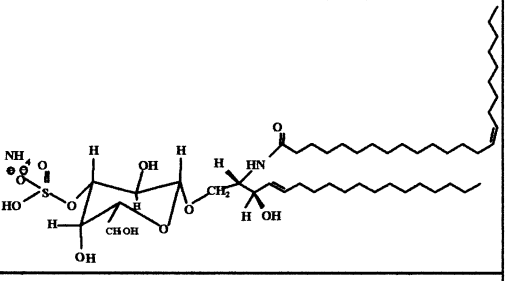 |
| Cholecystokinin Octapeptide (26-33)/CCK8, ($NH_4$ salt) | CCK8 | 1143.29 | *Sequence*: Asp-Tyr($SO_3H$) -Met-Gly-Trp-Met-Asp-Phe-$NH_2$ |

the improvement in ion signal using the monolayer substrate is due to the effective adsorption and isolation of the preformed LBPA ions on the protonated AET monolayer, thereby limiting analyte-analyte interactions and matrix effects that may limit sputter and ion yields.

During the course of the ion yield investigations we observed significant differences in the intensity of intact anion peaks relative to the $PO_2^-$ and $PO_3^-$ (from phospholipids) and $SO_3^-$ and $HSO_4^-$ (from organic sulfates) fragment ions generated from the thick and thin-layer targets by the atomic and polyatomic pri-

Table 2
Summary of the ion yields and intact-to-fragment ion ratios for the following phospholipids: OGP, LBPA, SOGP and DGPNB present as thick targets, and as thin targets on AET on Au; data were acquired using 20 keV $Cs^+$, and $(CsI)_2Cs^+$ primary ions; relative error of the mean for the ion yield measurements was measured to be ±5%

| *Thick Targets* | $Y_{M-}$ | $Y_{PO2-}$ | $Y_{PO3-}$ | $Y_{M-}/Y_{PO2-}$ | $Y_{M-}/Y_{PO3-}$ | Projectile |
|---|---|---|---|---|---|---|
| OGP | N.D. | 0.09% | 0.09% | ... | ... | $Cs^+$ |
| | N.D. | 1.4% | 4.3% | ... | ... | $(CsI)Cs^+$ |
| | N.D. | 2.4% | 5.6% | ... | ... | $(CsI)_2Cs^+$ |
| LBPA | 0.06% | 0.17% | 0.33% | 0.35 | 0.18 | $Cs^+$ |
| | 0.28% | 1.8% | 6.6% | 0.16 | 0.04 | $(CsI)Cs^+$ |
| | 0.28% | 3.0% | 7.4% | 0.09 | 0.04 | $(CsI)_2Cs^+$ |
| SOGP | 0.08% | 0.10% | 0.31% | 0.80 | 0.26 | $Cs^+$ |
| | 0.83% | 0.51% | 7.4% | 1.6 | 0.11 | $(CsI)Cs^+$ |
| | 0.73% | 2.2% | 7.7% | 0.33 | 0.09 | $(CsI)_2Cs^+$ |
| DGPNB | N.D. | 0.04% | 0.13% | ... | ... | $Cs^+$ |
| | N.D. | 0.78% | 3.3% | ... | ... | $(CsI)Cs^+$ |
| | N.D. | 1.3% | 3.0% | ... | ... | $(CsI)_2Cs^+$ |
| *Thin Targets* | $Y_{M-}$ | $Y_{PO2-}$ | $Y_{PO3-}$ | $Y_{M-}/Y_{PO2-}$ | $Y_{M-}/Y_{PO3-}$ | Projectile |
| OGP | 0.85% | 0.38% | 2.1% | 2.2 | 0.40 | $Cs^+$ |
| | 0.54% | 2.3% | 11% | 0.23 | 0.05 | $(CsI)Cs^+$ |
| | 0.48% | 3.9% | 13% | 0.12 | 0.04 | $(CsI)_2Cs^+$ |
| LBPA | 3.3% | 0.43% | 1.9% | 7.7 | 1.7 | $Cs^+$ |
| | 2.5% | 1.8% | 8.2% | 1.4 | 0.30 | $(CsI)Cs^+$ |
| | 0.88% | 1.8% | 7.1% | 0.49 | 0.12 | $(CsI)_2Cs^+$ |
| SOGP | 2.8% | 0.49% | 2.4% | 5.7 | 1.2 | $Cs^+$ |
| | 2.3% | 2.6% | 11% | 0.88 | 0.21 | $(CsI)Cs^+$ |
| | 3.2% | 2.8% | 8.6% | 1.1 | 0.37 | $(CsI)_2Cs^+$ |
| DGPNB | 2.6% | 0.41% | 2.3% | 6.3 | 1.1 | $Cs^+$ |
| | 2.3% | 1.6% | 9.3% | 1.4 | 0.24 | $(CsI)Cs^+$ |
| | 1.5% | 2.0% | 8.3% | 0.75 | 0.18 | $(CsI)_2Cs^+$ |

mary projectiles. A summary of the ion yields and intact-to-fragment ion yield ratios for the phospholipids (OGP, LBPA, SOGP, DGPNB) is provided in Table 2. A similar summary for the sulfated organic molecules (BS and CCK8) is provided in Table 3. Although each projectile produced more intact anion signal from the AET substrate, the polyatomic projectiles consistently generated higher relative fragment ion yields than the $Cs^+$ projectile at the same impact energy. It is clear from the data that regardless of the projectile complexity, the intact-to-fragment ion yield ratio is lower when sputtering from the solid salt target than from the AET monolayer. In the cases of OGP and DGPNB, no signal was detected from the thick targets. Tables 2 and 3 show secondary ion yields from different surfaces using a suite of projectiles. Intact ion yields increase from thick surfaces with polyatomic projectile impacts, but decrease from exchanged-AET surfaces. The fragment ion yields, however, increase for both thick and exchanged-AET surfaces.

Fig. 3 provides a comparison of the mass spectra produced by 20 keV $Cs^+$ projectile impacts on (a) LBPA thin layer on AET, (b) LBPA on a Au on Si blank (no monolayer present), and (c) LBPA on polished Si. In these cases, the adsorbed surfaces were prepared using procedure **(1)** (see Sec. 2). The ion intensities in each spectrum were corrected for the number of incident primary ions (ion doses are provided in the figure caption). The spectra in Fig. 3 demonstrate that the intensity of the intact LBPA anion is higher when sputtered from the AET monolayer surface. There is a factor of 20 increase in the intact ion yield from the LBPA deposited onto AET

Table 3
Summary of the ion yields and intact-to-fragment ion ratios for the following organic sulfates: BS and CCK8 present as thick targets, and as thin targets on AET on Au; data were acquired using 20 keV $Cs^+$, $(CsI)Cs^+$, and $(CsI)_2Cs^+$ primary ions; relative error of the mean for the ion yield measurements was measured to be ±5%

| *Thick Targets* | $Y_{M-}$ | $Y_{SO3-}$ | $Y_{HSO4-}$ | $Y_{M-}/Y_{SO3-}$ | $Y_{M-}/Y_{HSO4-}$ | Projectile |
|---|---|---|---|---|---|---|
| BS | 0.04% | N.D. | 0.11% | ... | 0.36 | $Cs^+$ |
| | 0.29% | N.D. | 1.5% | ... | 0.19 | $(CsI)Cs^+$ |
| | 0.40% | N.D. | 1.4% | ... | 0.29 | $(CsI)_2Cs^+$ |
| CCK8 | ≤0.007% | 0.20% | N.D. | ≤0.04 | ... | $Cs^+$ |
| | 0.12% | 4.1% | N.D. | 0.03 | ... | $(CsI)Cs^+$ |
| | 0.13% | 3.2% | N.D. | 0.04 | ... | $(CsI)_2Cs^+$ |
| *Thin Targets* | $Y_{M-}$ | $Y_{SO3-}$ | $Y_{HSO4-}$ | $Y_{M-}/Y_{SO3-}$ | $Y_{M-}/Y_{HSO4-}$ | Projectile |
| BS | 1.5% | N.D. | 1.7% | ... | 0.88 | $Cs^+$ |
| | 1.7% | N.D. | 6.2% | ... | 0.27 | $(CsI)Cs^+$ |
| | 1.2% | N.D. | 4.2% | ... | 0.28 | $(CsI)_2Cs^+$ |
| CCK8 | 0.45% | 2.0% | N.D. | 0.22 | ... | $Cs^+$ |
| | 0.30% | 5.2% | N.D. | 0.06 | ... | $(CsI)Cs^+$ |
| | 0.26% | 3.7% | N.D. | 0.07 | ... | $(CsI)_2Cs^+$ |

compared to a bare Au substrate, a factor of 530 increase compared to a polished Si surface, and a factor of 55 increase compared to LBPA deposited as a thick target. Table 4 shows similar intact ion yield improvements with 20 keV $Cs^+$ projectiles from various phospholipids and sulfated molecules. Similar yield improvements using AET over Au or polished Si substrates were also observed in our earlier study of the sputtering of adsorbed $BF_4^-$ and $B(C_6H_5)_4^-$ anions [11]. Polished Ag surfaces, commonly used in SIMS, were not relevant in these experiments as this substrate is employed to improve the cationization of molecules through the attachment of $Ag^+$.

Table 4
Summary of the ion yields for OGP, LBPA, SOGP, DGPNB, BS, and CCK8 present as thick targets, and as thin targets on polished Si surfaces, Au on Si, and AET monlayer on Au; data were acquired using 20 keV $Cs^+$ primary ions; relative error of the mean for the ion yield measurements was measured to be ±5%

| Molecule | Thick | Si | Au | AET |
|---|---|---|---|---|
| OGP | N.D | N.D. | 0.14% | 0.81% |
| LBPA | 0.06% | ≤0.006% | 0.17% | 3.2% |
| SOGP | 0.08% | ≤0.007% | 0.11% | 2.8% |
| DGPNB | N.D. | ≤0.002% | 0.24% | 2.5% |
| BS | 0.04% | ≤0.003% | 0.19% | 1.4% |
| CCK8 | ≤0.006% | N.D. | 0.08% | 0.41% |

### 3.2. Reversibility of phospholipid anion adsorption

We have previously shown that organic sulfates reversibly bind to an AET monolayer [12]. A series of experiments was conducted to investigate the adsorption reversibility for various phospholipids on an AET monolayer surface. Fig. 4 compares the negative ion mass spectra produced from the same AET monolayer following the application of LBPA and DGPNB [Fig. 4(a)], OGP and SOGP [Fig. 4(b)], and LBPA and DGPNB [Fig. 4(c)]. The spectra shown in Fig. 4 were generated using 20 keV $Cs^+$ projectiles at doses of $\sim 3 \times 10^4$ ions. Qualitatively similar spectra were produced from all surfaces by 20 keV $(CsI)_nCs^+$ ($n$ = 1–2) projectiles (spectra not shown). First, the AET monolayer was treated with a mixture of LBPA and DGPNB. The spectrum unambiguously shows in Fig. 4(a) that phospholipid anions have adsorbed to the protonated AET monolayer, as evidenced by the appearance of the LBPA and DGPNB intact ion peaks at *m/z* 666 and 854, respectively. There is also evidence of chloride ion at the surface due to peaks at *m/z* 35, 232, 267, 429, and 464 due to $Cl^-$, $AuCl^-$, $AuCl_2^-$, $Au_2Cl^-$, and $Au_2Cl_2^-$, respectively. We have previously shown that the intensities of these chloride-containing ions decrease upon the addition of

sulfates to the monolayer, thereby replacing some of the chloride-containing species [12].

The AET monolayer substrate was removed from the mass spectrometer, and the protocol outlined in the experimental section was used to rinse the substrate (thereby removing the anions adsorbed on the AET surface) and apply an OGP and SOGP phospholipid mixture. The mass spectrum in Fig. 4(b) shows that the HCl and chloroform rinse steps removed most of the chloride-containing ions (72% on average) and the LBPA and DGPNB anions (71% and 92% respectively) previously adsorbed to the AET monolayer. Additionally, OGP and SOGP (*m/z* 435 and 776) anions were exchanged to the surface by the second adsorption step.

The same monolayer substrate was removed from the instrument and rinsed according to protocol, and a mixture of LBPA and DGPNB was reapplied to the monolayer surface. The mass spectrum collected following the last adsorption step, shown in Fig. 4(c), indicates that well over 90% of OGP and SOGP anions were removed and that LBPA and DGPNB (*m/z* 666 and 854) were again adsorbed to the AET surface.

Based on these results, we conclude that the phospholipids are weakly bound to the AET monolayer and that the adsorption of inorganic ($Cl^-$) anions is also reversible. These experiments demonstrate that, provided low primary ion doses are used, the same AET monolayer can be used repeatedly to adsorb organic [and inorganic] anions for characterization by negative ion mode TOF-SIMS.

### *3.3. General utility of aminoethanethiol substrate*

The attractive aspect of substrate-enhanced secondary ion emission is the small number of projectiles required to obtain a mass spectrum. Fig. 5 shows a spectrum of LBPA adsorbed to an AET monolayer acquired in one minute using 20 keV $Cs^+$ projectiles at a dose of approximately $\sim 1 \times 10^3$ ions/cm$^2$. One nanomole of LBPA was applied to a 1 cm$^2$ AET substrate, then rinsed with chloroform (solvent) to insure submonolayer to monolayer coverage. The spectrum already shows the presence of the fragment peaks at *m/z* 63, 79, and 227 and the intact anion peak at *m/z* 666. At *m/z* 666, the signal-to-noise ratio is 10. Using only $10^3$ ions/cm$^2$ projectiles (on a 1 cm$^2$ target) means negligible surface damage is done to the surface, which is assumed to have $\sim 10^{14}$ molecules at monolayer coverage. Indeed, assuming each projectile causes damage to 100 surface molecules, then only $10^5$ surface molecules are damaged from $10^3$ primary ion impacts [16].

The limit of detection was tested by procedure **(2)** described in the experimental section. The concentration of the solutions was adjusted so that the total sample load applied to the AET surfaces included: 1nmol, 100 pmol, 10 pmol, 1 pmol, 100 fmol, and 1 fmol. In order to maintain the amount of LBPA adsorbed to the AET surfaces, no additional EtOH rinses were applied to the surfaces. The limit of detection under our experimental conditions is estimated at 10 pmol for LBPA.

## 4. Conclusions

We have shown that a suite of phospholipids and sulfates preferentially adsorbs to an AET self-assembled monolayer on Au. The AET substrate promotes significant increases in ion signal as generated by $(CsI)_nCs^+$ ($n = 0$–2) projectile bombardment, when compared to Au and Si blank substrates and to thick targets of their respective sodium or ammonium salts. The intact-to-fragment ion yield ratio is higher when sputtering from the AET monolayer target than from the solid salt. We attribute the improved performance of $Cs^+$ for sputtering intact negatively-charged ions from the AET surface to the fact that the anions are most likely sputtered by the intersection of single recoil cascades with the surface, a condition easily generated by atomic projectile impacts [11,12]. Further, we have demonstrated that the adsorption of these anions to an AET monolayer surface is reversible, so a single AET monolayer can be used repeatedly for anion adsorption and as a substrate for TOF-SIMS of anionic species. The substrate can be removed from the instrument and rinsed, thereby recollecting much of the original material from the surface for further use.

Advantages to using substrate-enhanced TOF-SIMS include: (1) No matrix additives are needed to absorb energy and affect ionization as in MALDI, thereby eliminating delayed extraction techniques to provide better resolution and high-accuracy measurements. (2) The AET method might be less destructive in terms of analyte fragmentation compared to fast-atom bombardment or MALDI because the "tethered" anion is easily liberated from the monolayer surface. The material adsorbed to the AET surface also binds reversibly, so it can be rinsed, collected, and reused once in solution again. (3) Due to very low primary ion fluences (in the event-by-event mode) needed to acquire a mass spectrum, very little of the sample is destroyed in the experiment. If the same number of primary ions ($10^3$–$10^5$) used in our experiment can be focused onto a smaller target size such as $10^4$ $\mu m^2$ ($1 cm^2$ in our experiment), then subpicomole detection limits are possible for molecules up to 1200 Daltons adsorbed to AET with "super"-static-TOF-SIMS. Substrate-enhanced TOF-SIMS may be a viable technique for the analysis of even larger biological molecules with fixed charge sites.

## Acknowledgement

This work was supported by the National Science Foundation (Grant CHE-9727474).

## References

[1] M.J. Van Stipdonk, R.D. Harris, E.A. Schweikert, Rapid Commun. Mass Spectrom. 10 (1996) 1987.
[2] R.D. Harris, M.J. Van Stipdonk, E.A. Schweikert, Int. J. Mass Spectrom. Ion Processes 174 (1998) 167.
[3] M. Benguerba, A. Brunelle, S. Della-Negra, J. Depauw, H. Joret, Y. Le Beyec, M.G. Blain, E.A. Schweikert, G. Ben Assayag, P. Sudraud, Nucl. Instrum. Methods Phys. Res. B 62 (1991) 8.
[4] A.D. Appelhans, J.D. Delmore, Anal. Chem. 61 (1989) 1087.
[5] G.S. Groenewold, J.E. Delmore, J.E. Olson, A.D. Appelhans, J.C. Ingram, D.A. Dahl, Int. J. Mass Spectrom. Ion Processes 163 (1997) 185.
[6] O.W. Hand, T.K. Majumdar, R.G. Cooks, Int. J. Mass Spectrom. Ion Processes 97 (1990) 35.
[7] W. Szymczak, K. Wittmaack, Nucl. Instrum. Methods Phys. Res. B 88 (1994) 149.
[8] S. Roberson, G. Gillen, Rapid Commun. Mass Spectrom. 12 (1998) 1303.
[9] F. Kötter, E. Niehuis, A. Benninghoven, in Secondary Ion Mass Spectrometry, SIMS XI, G. Gillen, R. Lareau, J. Bennett, F. Stevie (Eds.), Wiley, New York, 1998, p. 459.
[10] F. Kötter, A. Benninghoven, Appl. Surf. Sci. 133 (1998) 47.
[11] M.J. Van Stipdonk, R.D. English, E.A. Schweikert, J. Phys. Chem. B 103 (1999) 7929.
[12] M.J. Van Stipdonk, R.D. English, E.A. Schweikert, Anal. Chem. 72 (2000) 2618.
[13] R.D. English, M.J. Van Stipdonk, C.W. Diehnelt, E.A. Schweikert, Rapid Commun. Mass Spectrom. 15 (2001) 370.
[14] J.S. Patrick, R.G. Cooks, S.J. Pachuta, Biol. Mass Spectrom. 23 (1994) 653.
[15] M.E. Warren, A.H. Brockman, R. Orlando, Anal. Chem. 70 (1998) 3757.
[16] N. Winograd, Anal. Chem. 65 (1993) 622A.